2nd International Conference on
Modern Technologies in Sciences
13th March 2019

دومین کنفرانس بین المللی
فناوری های نوین در علوم
۲۲ اسفند ماه ۱۳۹۷

NONLINEAR DYNAMIC RESPONSE AND INSTABILITY ANALYSIS OF PIEZOELECTRIC NANOSHELL

Sayyid H. Hashemi Kachapi[*1] , Morteza Dardel[1] , Hamidreza Mohamadi daniali[1] , Alireza Fathi[1]
[1]Department of Mechanical Engineering, Babol Noshirvani University of Technology, P.O.Box484, Shariati Street, Babol, Mazandaran47148-71167, Iran
*corresponding author: sha.hashemi.kachapi@gmail.com

Abstract

In this paper, nonlinear vibration and frequency response and instability analysis of functionally graded piezoelastic cylindrical nanoshell (FG-PECNS) integrated with electrostatic excitation and Visco-Pasternak medium is investigated using the Gurtin–Murdoch surface/interface theory, von-karman-Donnell's shell model, Hamilton's principle and the assumed mode method combined with Lagrange–Euler's. Complex averaging method combined with arc-length continuation is used to achieve an approximate solution for nonlinear frequency response analysis. The validation and the parametric study are conducted on the nonlinear frequency response and instability analysis of the FG piezoelectric nanoresonator.

Keywords: FG-Piezoelastic nanoshell, Gurtin–Murdoch surface/interface theory, Nonlinear frequency and instability, Complex averaging method, Arc-length continuation, Electrostatic force.

1. INTRODUCTION

Recently, nano-scaled piezoelectric structures such as nano-beams, nano-membranes and nano-shells are attracting worldwide attention in nano-electro-mechanical (NEM) devices [1]. As a result, investigation on the piezoelectric nano-sized shell, for obtain the desired properties is crucial and this end, the vibration analysis should be addressed. Since the classical continuum theory cannot predict the surface and the size dependent response of nano-structures, some non-classical continuum theories such as the electro-elastic surface/interface Gurtin-Murdoch elasticity theory has been used to analyze the surface and the size dependent vibration of piezoelectric nano-structures [2, 3]. Recently, Fang et al. studied Size-dependent nonlinear vibration of nonhomogeneous shell embedded with a piezoelectric layer based on surface/interface theory [4]. Sun et al. used the both surface effects and nonlocal theory for buckling analysis of piezoelectric cylindrical nanoshells [5]. The size-dependent analysis of nonlinear buckling and postbuckling response and molecular dynamics simulation of FGM nanoshells are investigated by Sahmani et al. [6].
In the present study, nonlinear vibration and frequency response analysis of functionally graded piezoelastic cylindrical nanoshell (FG-PECNS) integrated with electrostatic excitation and Visco-Pasternak medium is investigated using the Gurtin–Murdoch surface/interface theory, von-karman-Donnell's shell model, Hamilton's principle and the assumed mode method combined with Lagrange–Euler's. Complex averaging method combined with arc-length continuation is used to achieve an approximate solution for nonlinear frequency response analysis. The validation and the parametric study are conducted on the nonlinear frequency response and instability analysis of the FG piezoelectric nanoresonator.

2. MATHEMATICAL FORMULATION

A cylindrical nano shell embedded with two piezoelectric layers and visco-Pasternak medium as nanoresonator is shown in Figure 1. The geometrical parameters of the cylindrical shell are the length of nano shell L, mid-surface radius R, thickness of cylindrical shell $2h_N$ thickness of piezoelectric material layer $2h_p$.

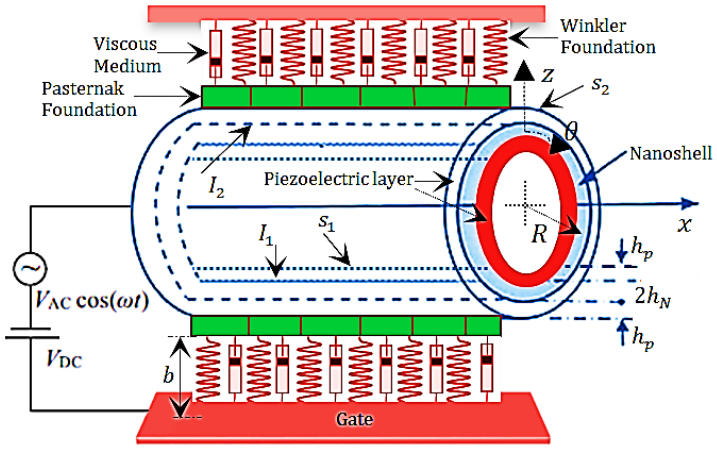

Fig. 1. *A piezoelastic cylindrical nano shell with surface/interface model*

2.1. Non- classical Shell theory and Governing equations

In the nano-shell and the piezoelectric layer, the constitutive relation can be expressed as [7, 8];

$$\begin{Bmatrix}\sigma_{xxN}\\ \sigma_{\theta\theta N}\\ \tau_{x\theta N}\end{Bmatrix}=\begin{bmatrix}C_{11N} & C_{12N} & 0\\ C_{21N} & C_{22N} & 0\\ 0 & 0 & C_{66N}\end{bmatrix}\begin{Bmatrix}\varepsilon_{xx}\\ \varepsilon_{\theta\theta}\\ \gamma_{x\theta}\end{Bmatrix},\ \begin{Bmatrix}\sigma_{xxp}\\ \sigma_{\theta\theta p}\\ \tau_{x\theta p}\end{Bmatrix}=\begin{bmatrix}C_{11p} & C_{12p} & 0\\ C_{21p} & C_{22p} & 0\\ 0 & 0 & C_{66p}\end{bmatrix}\begin{Bmatrix}\varepsilon_{xx}\\ \varepsilon_{\theta\theta}\\ \gamma_{x\theta}\end{Bmatrix}-\begin{bmatrix}0 & 0 & e_{31p}\\ 0 & 0 & e_{32p}\\ 0 & 0 & 0\end{bmatrix}\begin{Bmatrix}\bar{E}_{xp}\\ \bar{E}_{\theta p}\\ \bar{E}_{zp}\end{Bmatrix}, \quad (1)$$

With the radial component of electric field $\bar{E}_{zp}=V_p/h_{p2}$, the radial component of electric displacement D_{zp} can be presented as [9]

$$D_{zp}=e_{31p}\varepsilon_{xx}+e_{32p}\varepsilon_{\theta\theta}+\eta_{33p}\bar{E}_{zp} \quad (2)$$

With classical shell theory and the linear deflection and curvatures defined by Donnell's theory [7, 8], and based on the Gurtin–Murdoch surface/interface theory [2, 3], the normal stresses σ_x and σ_θ Eqs. (1) can be rewrite ten as

$$\sigma_{x(N,p)}=C_{11(N,p)}\varepsilon_x+C_{12(N,p)}\varepsilon_\theta+\frac{\upsilon_{(N,p)}\sigma_{zz(N,p)}}{1-\upsilon_{(N,p)}},\ \sigma_{\theta(N,p)}=C_{21(N,p)}\varepsilon_x+C_{22(N,p)}\varepsilon_\theta+\frac{\upsilon_{(N,p)}\sigma_{zz(N,p)}}{1-\upsilon_{(N,p)}},$$
$$\sigma_{x\theta(N,p)}=C_{66(N,p)}\gamma_{x\theta}, \quad (3)$$

Where

$$\sigma_{zz(N,p)}=\frac{z}{h_N+h_p}\left((\tau_0^{ps}+\tau_0^{NI})\left(\frac{\partial^2 w}{\partial x^2}+\frac{1}{R^2}\frac{\partial^2 w}{\partial\theta^2}\right)-(\rho^{ps}+\rho^{NI})\frac{\partial^2 w}{\partial t^2}\right) \quad (4)$$

2.2. Governing equations

In this section, the governing equations of the piezoelectric cylindrical nanoshell are obtained by applying the assumed mode method. With considering of the surface stress effect, the total strain and kinetic energies can be expressed as:

$$\pi=\frac{1}{2}\int_0^L\int_0^{2\pi}\left\{N_{xx}\varepsilon_{xx}^0+N_{\theta\theta}\varepsilon_{\theta\theta}^0+N_{x\theta}\gamma_{x\theta}^0+M_{xx}\kappa_{xx}+M_{\theta\theta}\kappa_{\theta\theta}+M_{x\theta}\kappa_{x\theta}+\eta_{33}\bar{E}_{zp}^2h_p\right\}Rd\theta dx\,. \quad (5)$$

$$T=\frac{1}{2}\iint I\left(\left(\frac{\partial u}{\partial t}\right)^2+\left(\frac{\partial v}{\partial t}\right)^2+\left(\frac{\partial w}{\partial t}\right)^2\right)Rd\theta dx \quad (6)$$

where the stresses and moment resultants and mass inertia are defined as:

$$\left(N_{ij(N,p)},M_{ij(N,p)}\right)=\int_{-h_N}^{h_N}\sigma_{ijN}(1,z)\,dz+\int_{-h_N-h_p}^{-h_N}\sigma_{ijp}(1,z)\,dz+\int_{h_N}^{h_N+h_p}\sigma_{ijp}(1,z)\,dz+2\sigma^{s,I}, \quad (7)$$

$$I=\int_{-h_N}^{h_N}\rho_N\,dz+\int_{-h_N-h_p}^{-h_N}\rho_p\,dz+\int_{h_N}^{h_N+h_p}\rho_p\,dz+\rho^{s,I}=2\rho_Nh_N+2\rho_ph_p+2\rho^{ps}+2\rho^{NI} \quad (8)$$

Where the stresses and moment resultants are defined as following:

$$N_{xx}=A_{11}\varepsilon_{xx}^0+A_{12}\varepsilon_{\theta\theta}^0-(\tau_0^s+\tau_0^I)\left(\frac{\partial w}{\partial x}\right)^2+2(\tau_0^{ps}+\tau_0^{NI})-N_{xp} \quad (9a)$$

$$N_{\theta\theta}=A_{21}\varepsilon_{xx}^0+A_{22}\varepsilon_{\theta\theta}^0-\left(\tau_0^{ps}+\tau_0^{NI}\right)\left(\frac{2w}{R}+\frac{1}{R^2}\left(\frac{\partial w}{\partial\theta}\right)^2\right)+2(\tau_0^s+\tau_0^I)-N_{\theta p}, \quad (9b)$$

$$N_{x\theta}=A_{66}\gamma_{x\theta}^0, \quad (9c)$$

$$M_{xx} = D_{11}\kappa_{xx} + D_{12}\kappa_{\theta\theta} - M_{xp} + E_{11}^{*}\left(\frac{\partial^2 w}{\partial x^2} + \frac{1}{R^2}\frac{\partial^2 w}{\partial \theta^2}\right) - G_{11}^{*}\frac{\partial^2 w}{\partial t^2}, \quad (9d)$$

$$M_{\theta\theta} = D_{21}\kappa_{xx} + D_{22}\kappa_{\theta\theta} - M_{\theta p} + E_{11}^{*}\left(\frac{\partial^2 w}{\partial x^2} + \frac{1}{R^2}\frac{\partial^2 w}{\partial \theta^2}\right) - G_{11}^{*}\frac{\partial^2 w}{\partial t^2}, \quad (9e)$$

$$M_{x\theta} = D_{66}\kappa_{x\theta}, \quad (9f)$$

The kinetic energy of the nanoshell may be written as:

$$T = \frac{1}{2}\iint\left\{I\left(\left(\frac{\partial u}{\partial t}\right)^2 + \left(\frac{\partial v}{\partial t}\right)^2 + \left(\frac{\partial w}{\partial t}\right)^2\right)\right\} Rd\theta dx \quad (10)$$

The work done by the potential due to external electric voltage, visco-pasternak effect and electrostatic force respectively, can be expressed as [10, 11]

$$W_p = \frac{1}{2}\int_0^L\int_0^{2\pi}(N_{xp}(\partial w/\partial x)^2 + (1/R^2)N_{\theta p}(\partial w/\partial\theta)^2)\, Rd\theta dx, \quad (11)$$

$$W_{vm} = -\int_0^L\int_0^{2\pi}\int_0^w (K_w w - K_p\nabla^2 w + C_w\frac{\partial w}{\partial t})dw\, Rd\theta dx \quad (12)$$

$$W_e = \int_0^L\int_0^{2\pi}\int_0^w \frac{\pi\Upsilon(V_{DC} + V_{AC}\cos(\omega t))^2}{\sqrt{(b-w)(2R+b-w)}\left[\cosh^{-1}\left(1+\frac{b-w}{R}\right)\right]^2} dw\, Rd\theta dx \quad (13)$$

where the air permittivity is $\Upsilon = 8.85\times10^{-12}C^2N^{-1}m^{-2}$ [11].

for discretizing equations of motion, the assumed mode method combined with Lagrange–Euler's is used. using following dimensionless parameters for Eqs. (5-13)

$$\begin{aligned}
&(\bar{u},\bar{v},\bar{w}) = \frac{(u,v,w)}{h_N}, \xi = \frac{x}{L}, \left(\bar{A}_{ij},\bar{B}_{ij},\bar{D}_{ij}\right) = \frac{\left(A_{ij},B_{ij},D_{ij}\right)}{A_{11N}(1,h_N,h_N^2)}, \bar{\tau}_0^{s(i,o)} = \frac{\tau_0^{S(i,o)}}{A_{11N}}, m_0 = \frac{L}{R}, m_1 = \frac{L}{h_N},\\
&\left(\bar{A}_{ij}^{*},\bar{B}_{ij}^{*},\bar{D}_{ij}^{*}\right) = \frac{\left(A_{ij}^{*},B_{ij}^{*},D_{ij}^{*}\right)}{A_{11N}(1,h_N,h_N^2)}, (\bar{F}_{11}^{*},\bar{E}_{11}^{*}) = \frac{(F_{11}^{*},E_{11}^{*})}{A_{11N}(h_N,h_N^2)}, \bar{N}_{(x,\theta)p2}^{*} = \frac{N_{(x,\theta)p2}^{*}}{A_{11N}}, \bar{h}_p = \frac{h_p}{R},\\
&\bar{M}_{(x,\theta)p2}^{*} = \frac{M_{(x,\theta)p2}^{*}}{A_{11N}h_N}, m_2 = \frac{h_N}{R} = \bar{h}_N, m_3 = \frac{I}{2\rho_N h_N}, \Omega = \sqrt{\frac{A_{11N}}{2\rho_N h_N L^2}}, \tau = \Omega t, \bar{\Omega} = \frac{\omega}{\Omega}, m_4 = \frac{h_p}{h_N},\\
&\bar{K}_{(w,p)} = \frac{K_{(w,p)}(L^2,1)}{m_3 A_{11N}}, \bar{J}_{11}^{*} = \frac{J_{11}^{*}}{\rho_N h_N^2}, \bar{G}_{11}^{*} = \frac{G_{11}^{*}}{\rho_N h_N^3}, \bar{C}_w = \frac{C_w\Omega L^2}{m_3 A_{11N}}, \bar{V}_{DC}^{AC} = \frac{V_{DC}^{AC}}{V_0}, \bar{F}_e = \frac{\pi m_1 V_0^2\Upsilon}{m_3 A_{11N}},
\end{aligned} \quad (14)$$

and displacement in terms of generalized coordinate and mode function reference [8] and substituting into dimensionless strain and kinetic energies and works and applying the Euler–Lagrange method results in the following reduced-order model of the system:

$$[(M)_u^u]\{\ddot{\bar{u}}\} + [(K)_u^u]\{\bar{u}\} + [(K)_u^v]\{\bar{v}\} + [(K)_u^w]\{\bar{w}\} + [(NL)_u^w]\{\bar{w}^2\} = \bar{F}_{up}, \quad (15)$$

$$[(M)_v^v]\{\ddot{\bar{v}}\} + [(K)_v^u]\{\bar{u}\} + [(K)_v^v]\{v\} + [(K)_v^w]\{\bar{w}\} + [(NL)_v^w]\{\bar{w}^2\} = \bar{F}_{vp}, \quad (16)$$

$$\begin{aligned}
&[(M)_w^w]\{\ddot{\bar{w}}\} + [(c)_w^w]\{\dot{\bar{w}}\} + [(K)_w^u]\{\bar{u}\} + [(K)_w^v]\{\bar{v}\} + [(K)_w^w - \bar{F}_{e2}(K_e)_w^w]\{\bar{w}\} + [(NL)_w^u]\{\bar{w}\bar{u}\}\\
&+[(NL)_w^v]\{\bar{w}\bar{v}\} + [(NL)_{w2}^w - \bar{F}_{e3}(NL_{2e})_w^w]\{\bar{w}^2\} + [(NL)_{w3}^w - \bar{F}_{e4}(NL_{3e})_w^w]\{\bar{w}^3\} = \bar{F}_{we} + \bar{F}_{wp}\\
&+\bar{F}_e\{((\bar{V}_{AC}cos\bar{\omega}\tau)^2 + 2\bar{V}_{AC}\bar{V}_{DC}cos\bar{\omega}\tau)(\bar{C}_4(NL_{3e})_w^w + \bar{C}_3(NL_{2e})_w^w + \bar{C}_2(K_e)_w^w + \bar{C}_1\bar{F}_1)\}
\end{aligned} \quad (17)$$

where $(M), (c)$ and (K) are mass, damping and linear stiffness matrixes. $(NL)_u^w, (NL)_v^w$, and $(NL)_{w2}^w$ are second-order nonlinear stiffness matrixes and $(NL)_{w3}^w$ is third-order nonlinear stiffness matrix. Also, K_e, NL_{2e} and NL_{3e} are the linear stiffness, second and third order nonlinear stiffness matrixes for electrostatic force expansion, respectively, and also, $\bar{F}_{up}$, $\bar{F}_{vp}$ and $\bar{F}_{wp}$ are applied loads by piezoelectric voltage and surface stress.

3. ANALYTICAL SOLUTIONS, RESULTS AND DISCUSSIONS

In this section, the nonlinear frequency response of FG-PECNS is solved by Complex averaging method combined with arc-length continuation [12, 13]. The material properties for nonhomogeneous nano-shell and piezoelectric layer are shown in Table 1-2, respectively [10, 14].

Table 1: *Properties of stainless steel and nickel [10, 14]*

Stainless steel			Nichel		
$E_B(GPa)$	υ_B	$\rho_B(kg\,m^{-3})$	$E_T(GPa)$	υ_T	$\rho_T(kg\,m^{-3})$
208	0.381	8166	205	0.31	8900

Table 2. *Properties of PZT-4 [14, 18]*

$E_p(GPa)$	υ_p	$e_{31p}(C/m^2)$	$e_{32p}(C/m^2)$	$\eta_{33p}(10^{-11}F/m)$	$\rho_p(kg\,m^{-3})$

95	0.3	−5.2	−5.2	560	7500

The material and geometrical parameters used in all following results are shown in Table 3 [10, 14].

Table 3: *The material and geometrical parameters [10, 14]*

$R(m)$	L/R	h_N/R	h_p/R	$\lambda^{SI}(N/m)$	$\mu^{SI}(N/m)$	$\tau_0^{SI}\ (N/m)$
1×10^{-9}	10	0.02	0.02	4.488	2.774	0.6
$\rho^{SI}(kg/m^2)$	$V_p(V)$	$\lambda^{sp}(N/m)$	$\mu^{sp}(N/m)$	$\tau_0^{sp}(N/m)$	$e_{31p}^{sp}(C/m)$	$e_{32p}^{sp}(C/m)$
3.17×10^{-7}	1×10^{-5}	4.488	2.774	0.6	-3×10^{-8}	-3×10^{-8}
$\rho^{sp}(kg/m^2)$	$C_w(N.S/m)$	$K_w(N/m^3)$	$K_p(N/m)$	$V_{AC}(V)$	$V_{DC}(V)$	b/R
5.61×10^{-6}	5×10^{-9}	1×10^{15}	1×10^{-2}	3	1	2

3.1. Effects of PECNS parameters on nonlinear system response

The main purpose of this section is obtaining analytical solutions of equation for nonlinear frequency response, based on arc-length continuation method and instability analysis. The frequency responses of the piezoelectric nano-shell for different boundary conditions (SS, CC, CS and CF) are presented in Figure 2. It can be seen that the SS boundary condition has maximum resonance amplitude, and is the only boundary condition that instability occurs with saddle-node bifurcations and the rest of the boundary conditions are stable.

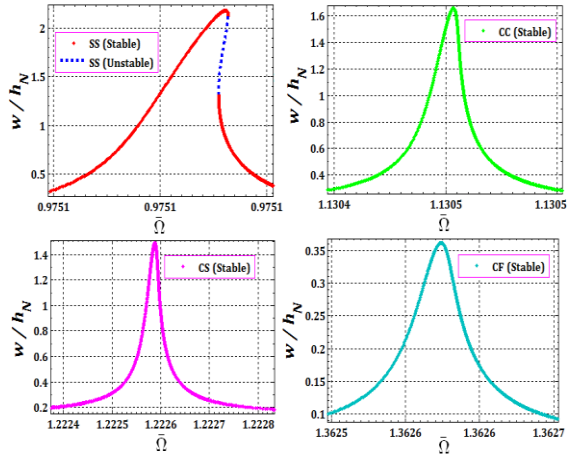

Fig. 2. *The effect of different boundary conditions on the frequency response of the SS FG-PECNS*

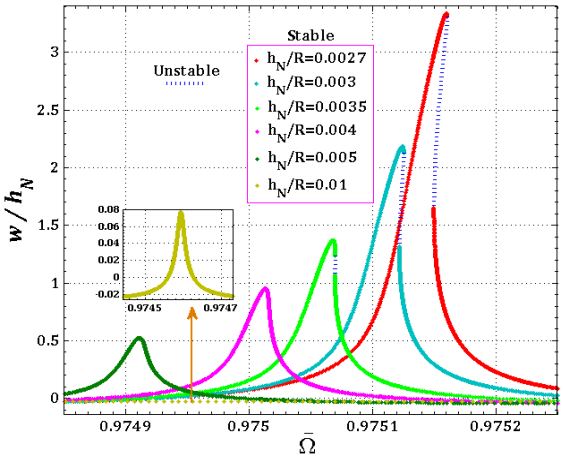

Fig. 3. *The effect of h_N/R on frequency response of SS FG-PECNS*

Figure 3 show the effects of the ratio nanoshell thickness h_N/R on the nonlinear frequency response and stability analysis of the SS FG-PECNS. It can seen that with increasing h_N/R ratio, the resonance frequencies and the oscillation amplitude decreases and the system becomes stable and the range of instability with saddle-node bifurcations decreases and the nonlinear hardening behaviour becomes weaker and the nonlinear resonance occurs at lower excitation frequencies and smaller transverse amplitudes.

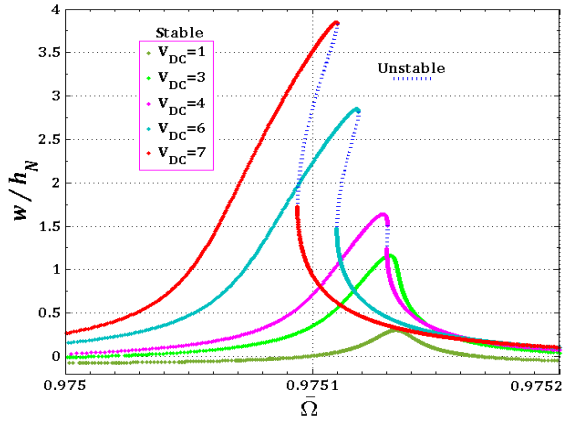

Fig. 4. *The effect of direct voltage V_{DC} on frequency response of SS FG-PECNS*

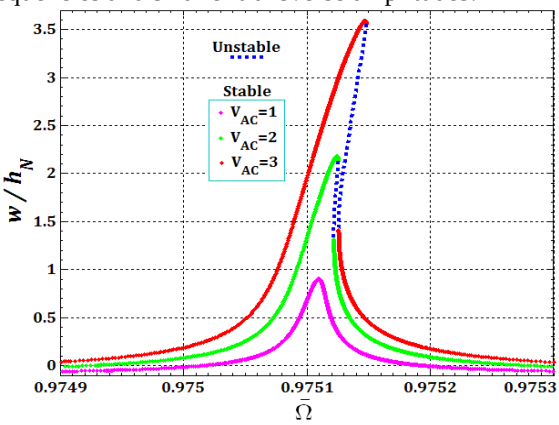

Fig. 5. *The effect of alternating voltage V_{AC} on frequency response of SS FG-PECNS*

In Figures 4 and 5, the effects of different direct electric voltage (V_{DC}) and alternating electric voltage (V_{AC}) on the frequency response respectively are shown. The results show that with increasing of both voltages V_{DC} and V_{AC}, the oscillation amplitude is increase. Moreover, due to increased amplitude of the DC voltage (and hence increased amplitude of the static deflection) and also AC voltage, the system displays hardening-type nonlinear behaviour with two saddle-node bifurcations.

4. CONCLUSION

In current study, nonlinear vibration and frequency response analysis of functionally graded piezoelastic cylindrical nanoshell (FG-PECNS) integrated with electrostatic excitation and Visco-Pasternak medium is investigated using the Gurtin–Murdoch surface/interface theory, von-karman-Donnell's shell model, Hamilton's principle and the assumed mode method combined with Lagrange–Euler's. Complex averaging method combined with arc-length continuation is used to achieve an approximate solution for nonlinear frequency response analysis. The validation and the parametric study are conducted on the nonlinear frequency response and instability analysis of the FG piezoelectric nanoresonator.

Some conclusions are obtained from this study:

- SS boundary condition has maximum resonance amplitude and instability occurs with saddle-node bifurcations and the rest of the boundary conditions are stable.
- with increasing h_N/R ratio, the resonance frequencies and the oscillation amplitude decreases and the system becomes stable and the range of instability with saddle-node bifurcations decreases and the nonlinear hardening behaviour becomes weaker.
- with increasing of both voltages V_{DC} and V_{AC}, the oscillation amplitude is increase. Moreover, due to increased amplitude of the DC and AC voltages, the system displays hardening-type nonlinear behaviour with two saddle-node bifurcations.

REFERENCES

[1] Jalili, N. (2010). Piezoelectric-Based Vibration Control: From Macro to Micro/Nano Scale Systems, *Springer*, New York.

[2] Gurtin, M.E., & Murdoch, A.I. (1975). A continuum theory of elastic material surface. *Archive for Rational Mechanics and Analysis*, 57(4), 291–323.

[3] Gurtin, M.E., & Murdoch, A.I. (1978). Surface stress in solids. *International Journal of Solids and Structures*, 14(6), 431–40.

[4] Fang, X.Q., Liu, J.X., & Gupta, V. (2013). Fundamental formulations and recent achievements in piezoelectric nano-structures: a review, *Nanoscale*, 5(5), 1716–26.

[5] Sun, J., Wang, Z., Zhou, Z., Xu, X., & Lim, C.W. (2018). Surface effects on the buckling behaviors of piezoelectric cylindrical nanoshells using nonlocal continuum model. *Applied Mathematical Modelling*, 59, 341-356.

[6] Sahmani, S., Aghdam, M.M., & Bahrami, M. (2017). An efficient size-dependent shear deformable shell model and molecular dynamics simulation for axial instability analysis of silicon nanoshells. *Journal of Molecular Graphics and Modelling*, 77, 263-279.

[7] Donnell, L.H. (1976). Beam, Plates and Shells, *McGraw-Hill*, New York.

[8] Amabili, M. (2008). Nonlinear Vibrations and Stability of Shells and Plates, *Cambridge University Press*, New York.

[9] Sabzikar Boroujerdy, M., & Eslami, M.R. (2014). Axisymmetric snap-through behavior of Piezo-FGM shallow clamped spherical shells under thermo-electro-mechanical loading, *International Journal of Pressure Vessels and Piping*, 120-121, 19-26.

[10] Ghorbanpour Arani, A., Kolahchi, R., & Hashemian, M. (2015). Nonlocal surface piezoelasticity theory for dynamic stability of double-walled boron nitride nanotube conveying viscose fluid based on different theories. *Proceedings of the Institution of Mechanical Engineers, Part C: Journal of Mechanical Engineering Science*, DOI: 10.1177/0954406214527270.

[11] Farokhi, H., Païdoussis, M.P., & Misra, A. (2016). A new nonlinear model for analyzing the behavior of carbon nanotube-based resonators, *Journal of Sound and Vibration*, 378, 56-75.

[12] Manevitch, A.I., & Manevitch, L.I., (2005). Themechanics of Nonlinear Systems with Internal Resonance, *Imperial College Press*, London.

[13] Parseh M., Dardel, M., & Ghasemi, M.H., Pashaei, M.H. (2016). Steady state dynamics of a non-linear beam coupled to a non-linear energy sink, *International Journal of Non-Linear Mechanics*, 79, 48–65.

[14] Jafari, A.A., Khalili, S.M.R., & Tavakolian, M. (2014). Nonlinear vibration of functionally graded cylindrical shells embedded with a piezoelectric layer, *Thin Wall Structures*, 79, 8–15.